Gondwana Research, V. 6, No. 4, pp. 757-765.

ISSN: 1342-937X

GR Gondwana Research

Petrology and Geochemistry of the Volcanic Rocks Dredged from the Geophysicist Seamount in the Kurile Basin: Evidence for the Existence of Thinned Continental Crust

Igor A. Tararin[1], Eugeniy P. Lelikov[2] and Reinhard Werner[3]

[1] *Far East Geological Institute, Russian Academy of Sciences, Vladivostok 690022, Russia, E-mail: tararin@fegi.ru*

[2] *Il'ichev Pacific Institute of Oceanology, Russian Academy of Sciences, Vladivostok 690041, Russia, E-mail: pacific@online.marine.su*

[3] *Tethys Geoconsulting GmbH, Wischhofstr. 1-3, D-24148, Kiel, Germany, E-mail: rwerner@geomar.de*

(Manuscript received July 22, 2002; accepted May 6, 2003)

Abstract

Dredged samples from the Geophysicist seamount volcano in the northeastern part of the Kurile Basin include volcanic and volcanoclastic rocks ranging from basalt to andesite. The rocks have geochemical features typical of high-K island-arc calc-alkaline volcanism. They are enriched in LILE and depleted in Zr, Ti, Nb, Ta and Y. The chondrite-normalized REE patterns are characterized by enrichment of LREE similar to those of island-arc lava from the submarine volcanoes of rear-arc zone of the Kurile Island Arc. The volcanic rocks have a wide range of $^{87}Sr/^{86}Sr$ ratios (0.70287-0.70652), varying $^{143}Nd/^{144}Nd$ and Pb isotopic ratios. Their trace-element compositions and Sr-Nd-Pb isotope signatures may be explained by a small addition of crustal continental component to mantle-derived magmas that suggest the existence of thinned continental basement under the eastern part of the Kurile Basin.

Key words: Geophysicist seamount volcano, geochemistry, interaction of basic magma with thinned continental crust, Kurile Basin, Sea of Okhotsk.

Introduction

Bound the Asian continent in the north and northwest and the Kurile-Kamchatka Island Arc in the east and southeast, the marginal Sea of Okhotsk has a complex and heterogeneous basement structure (Geodekyan et al., 1976; Gnibidenko, 1979; Sergeev et al., 1987; Bogdanov, 1988; Frolova et al., 1989; Avdeiko et al., 1992; Lelikov, 1992; Baranov et al., 1999; Bogdanov and Dobretsov, 2002).

The Kurile Basin in the Sea of Okhotsk is a back-arc basin located behind the Kurile Island Arc. The basement structure of the basin has been studied insufficiently. The most reliable data are based on sediments, whereas the composition and origin of the acoustic basement is practically unknown. Direct evidence for the age of the Kurile Basin floor is lacking, as no magnetic lineations have been found inside the basin and the basin crust has not been sampled directly by drilling. Basing on the heat flow data, basement depth, seismo-stratigraphy, and investigation the adjacent land magmatism, the basin was postulated to have formed by back-arc spreading in early Oligocene to Middle Miocene (32-15 Ma) (Kimura and Tamaki, 1986; Kharakhinov, 1996; Hayashi, 1997) or from early Miocene to late Miocene (~23-8 Ma) (Takeuchi et al., 1999; Ikeda et al., 2000).

Therefore the main goal of the joint German-Russian Project 'Kurile-Okhotsk Marine EXperiment' (KOMEX) is to obtain petrological and geochemical data to trace the origin of the Kurile Basin basement.

Morphology and Crustal Structure of the Kurile Basin

The Kurile Basin being of a triangular shape and strikes in a NE-SW direction (Fig. 1). It is approximately 700 km in length and has a maximum width of about 250 km in the southwest, narrows northeastward. The average depth of the basin is 3000 m; its maximal depth amounts to 3374 m b.s.l. (below sea level).

Seismic refraction studies show that the crust of the southwestern Kurile Basin begins with a thick (up to 5 km) sedimentary blanket with a compressional wave velocity of 1.7–4.3 km/s. This is underlain by a 4.8–5.2 km/s layer 2.0–2.8 km thick, presumably representing the upper consolidated, volcanogenic-sedimentary section of oceanic crust (layers 1 and 2). The underlying high-velocity layer 4–5 km thick (6.4–7.2 km/s) corresponds to oceanic layer 3 (Snegovskoy, 1974; Belousov and Udintsev, 1981; Sergeev et al., 1987; Neprochnov et al., 1999). The Moho discontinuity that occurs at 11–13 km below sea level and the upper mantle is characterized by seismic velocities up to 8 km/s (Bikkenina et al., 1987; Gnibidenko et al., 1995). Data on the crustal structure of the northeastern part of the basin are absent.

The southeastern margin of the Kurile Basin has a complex structure, due to many seamounts aligned in the form of an *en echelon* ridges striking into the basin at angles of about 25–90° to the general trend of the Kurile Arc (Fig. 1) (Avdeiko et al., 1992). These seamounts occur as discrete volcanic edifices or volcanic ridges (Gnibidenko et al., 1995), which extend into the Kurile Basin for tens of kilometers (Fig. 1). All of these structures are covered by sediments and are thus inaccessible to sampling by dredging. The only known exception is the Geophysicist seamount volcano (Gnibidenko and Svarichevsky, 1984) at the northeastern end of the Kurile Basin abyssal plain (Fig. 1), which has ~5.5–6.5 km in diameter and rises from the basement (3200 m.b.s.l.) to the depth of 2370 m b.s.l. This volcanic edifice was investigated in detail during several cruises of the KOMEX Project (Nürnberg et al., 1997; Biebow and Hütten, 1999; Biebow et al., 2000) (Table 1).

Geophysicist Seamount Volcano

Introduction and geologic setting

The dredging samples (Table 1) comprise mostly angular blocks and fragments of pillow-like lavas or brecciated basalt and basaltic andesite and even scoriaceous fragments and other volcanoclastic rocks, ranging from some centimeter to more than 0.5 m in size. The surface of boulders and blocks is very rough. Usually they are slightly weathered and rare hydrothermally altered, sometimes with thin (up to 3-4 cm) sedimentary and Mn-oxide coating.

Petrography and mineralogy

The submarine volcano is made of highly porphyritic (up to 20-30% phenocryst), vesicular in appearance (up to 50 vol.% vesicles), inclusion-rich, basalt, basaltic andesite and subordinate andesite.

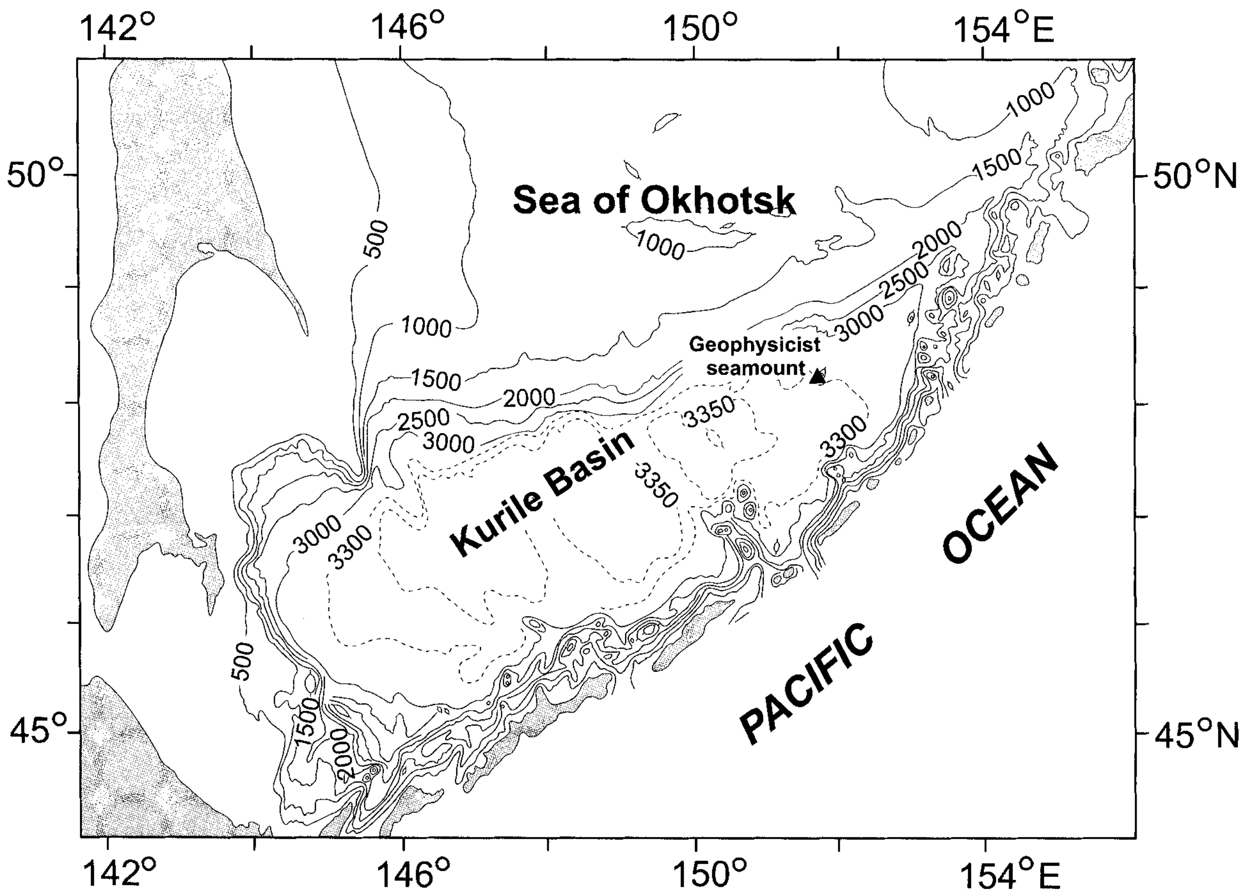

Fig. 1. Bathymetry of the Kurile Basin. Depth contour interval is 500 m. Triangle indicates Geophysicist Seamount volcano.

Table 1. Location of the Kurile Basin Geophysicist submarine volcano dredges and rock recovery; RV Akademik Lavrentyev cruise 27 and 28 and RV Marshal Gelovany cruise 1999.

Dredge	Latitude Begin/End	Longitude Begin/End	Water depth, m	Rock types recovered
LV27-18	48°19.480'/ 48°19.060'	151°50.130'/ 151°50.240'	3190-2945	Basaltic andesite, dropstones
LV28-45	48°18.141'/ 48°18.421'	151°48.684'/ 151°49.317'	2700-2450	Basalt, dropstones
LV28-47	48°18.409'/ 48°18.814'	151°49.079'/ 151°49.520'	2450-2400	Sediment, dropstones
LV28-48	48°17.852'/ 48°17.690'	151°49.017'/ 151°49.238'	2900-2980	Basalt, andesite, dropstones, sediment
LV28-49	48°18.790'/ 48°18.570'	151°49.485'/ 151°48.854'	2500-2470	Sediment, dropstones
LV28-56	48°18.486'/ 48°18.137'	151°48.942'/ 151°50.197'	2500-2774	Fresh and hydrothermally altered basalt, basaltic andesite, barite, dropstones
GE99-39	48°18.570'/ 48°19.180'	151°48.950'/ 151°49.100'	2940-2740	Fresh and hydrothermally altered basalt, dropstones

In basalt, the phenocrysts are plagioclase, clinopyroxene, olivine, and amphibole; glomerocrysts of plagioclase and plagioclase-augite are abundant. Individual phenocrysts are usually 1-4 mm in size, but the predominant crystal size is 0.5-1.0 mm. Plagioclase is usually the most abundant phenocryst phase and generally displays complex oscillatory zoning, with an overall trend from calcic cores (An_{93-70}, Table 2) to sodic rims (An_{60-65}) and may contain numerous glass inclusions.

Clinopyroxene is second to plagioclase as a major phenocryst phase and is the most common groundmass pyroxene. Clinopyroxene is predominantly of Ca-rich augite (Table 2) but some diopside or salite. Olivine phenocrysts range in composition from Fo_{89} to Fo_{76} and tend to disappear in rocks with SiO_2>54% where it is replaced by orthopyroxene. Brown-green hornblende phenocrysts are typical both of basalt and more evolved basaltic andesite and are represented by magnesio-hastingsite, magnesian hastingsite hornblende or rare pargasite (after Leake, 1978). Phenocrysts of Fe-Ti-oxides are magnetite and titanomagnetite. The groundmass is mainly composed of fresh or slightly altered glass with numerous plagioclase (An_{60-83}) microlites as well as Ca-rich pyroxene, Fe-Ti-oxides and occasionally olivine in varying amounts.

Phenocryst assemblages of basaltic andesite, in decreasing proportions, are plagioclase feldspar (An_{89-65}, Table 2), augite, brown-green tschermakitic or pargasitic hornblende, orthopyroxene (En_{69-73}) and minor olivine (Fo_{83-73}). The groundmass consists mainly of glass containing plagioclase (An_{50-70}) laths together with variable proportions of Ca-rich pyroxene, orthopyroxene, amphibole and Fe-Ti-oxides.

Analytical methods

Mineral compositions were obtained using CAMECA SX50 electron microprobe at the GEOMAR Research Center and CAMEBAX electron microprobe at the Institute Volcanology Russian Academy of Sciences. Natural minerals and glass were used as standards for most elements.

Samples selected for geochemistry were carefully hand-picked under a binocular microscope. Major and some trace elements (e.g., Cr, Ni, Zr, Sr) of whole rocks were determined on fused beads using the Phillips X'Unique PW1480 X-ray fluorescence spectrometer (XRF) equipped with Rh-tube at GEOMAR. Additional trace elements (e.g., Rb, Ba, Y, Nb, Ta, Hf, U, Th and all REE's) were determined by ICP-MC at Activation Laboratories Ltd. (Ontario, Canada; for analytical procedures see www.actlabs.com).

Samples for Sr-Nd-Pb isotopic analyses were leached with hot 6N HCl to minimize the effects of seawater alteration. Chemical separation procedures for Sr, Nd and Pb are described in Hoernle and Tilton (1991). Sr, Nd and Pb isotope ratios were determined on Finnigan MAT 262-RPQ2+ at GEOMAR. Replicate analyses of Sr-Nd-Pb isotopes on the same samples were within the analytical uncertainties. Sr was measured in static mode and $^{87}Sr/^{86}Sr$ was normalized within run to $^{86}Sr/^{88}Sr$=0.1194. The long-term average value of NBS987 gave $^{87}Sr/^{86}Sr$ ratio of 0.710254±0.000017 (N=83; all reported errors are ±2σ). The $^{143}Nd/^{144}Nd$ ratio was normalized within run to $^{146}Nd/^{144}Nd$=0.7219 and measured in static mode. The La Jolla standard yielded a long-term average for $^{143}Nd/^{144}Nd$ of 0.511845±0.000011 (N=123). All Pb analyses were corrected to NBS981 (Todt et al., 1996) for fractionation.

Table 2. Representative microprobe analyses of mineral in basalt, basaltic andesite and andesite from the Geophysicist seamount volcano.

	LV28-48-1f													LV28-56-1-3	
	$Ol^{I}c$	$Ol^{I}r$	Cpx^{I}_{c}	Cpx^{I}_{r}	Hb^{I}_{c}	Hb^{I}_{r}	Pl^{I}_{c}	Pl^{I}_{r}	Ol^{II}_{c}	Ol^{II}_{r}	Cpx^{II}_{c}	Cpx^{II}_{r}	Pl^{II}_{r}	Ol^{I}_{c}	Ol^{I}_{r}
SiO_2	39.72	38.87	51.73	49.46	40.65	39.92	46.00	50.82	40.55	39.74	48.43	48.96	53.41	40.61	40.88
TiO_2	0.00	0.00	0.49	1.35	2.44	2.99	0.00	0.05	0.00	0.03	1.16	1.49	0.05	n.d.	n.d.
Al_2O_3	0.00	0.00	3.69	5.99	13.96	13.99	34.74	30.72	0.00	0.00	6.93	6.36	29.13	n.d.	n.d.
Cr_2O_3	0.00	0.00	0.58	0.00	0.00	0.00	0.00	0.00	0.00	0.00	0.00	0.00	0.00	n.d.	n.d.
FeO	12.97	22.09	4.08	8.10	12.53	11.31	0.61	0.89	12.47	21.61	8.11	8.69	0.90	12.74	11.27
MnO	0.02	0.22	0.00	0.04	0.09	0.00	0.00	0.00	0.05	0.30	0.00	0.02	0.00	n.d.	n.d.
MgO	47.23	39.84	16.26	13.06	14.23	13.95	0.00	0.00	45.92	37.83	12.79	12.84	0.00	47.33	48.55
NiO	0.03	0.00	0.00	0.00	0.00	0.00	0.00	0.00	0.00	0.00	0.00	0.00	0.00	0.11	0.20
CaO	0.21	0.23	23.69	21.89	11.32	11.70	17.84	13.60	0.17	0.23	20.98	21.01	11.75	n.d.	n.d.
Na_2O	0.00	0.00	0.03	0.48	2.39	2.36	1.35	4.02	0.00	0.01	0.26	0.44	4.12	n.d.	n.d.
K_2O	0.03	0.01	0.03	0.05	1.00	1.17	0.08	0.32	0.02	0.02	0.07	0.04	0.42	n.d.	n.d.
Total	100.21	100.26	100.58	100.42	98.52	97.39	100.62	100.42	99.18	99.77	98.73	99.85	99.78	100.79	100.90
X_{Mg}	0.867	0.763	0.877	0.742	0.669	0.687	-	-	0.868	0.757	0.738	0.725	-	0.869	0.885
X_{An}	-	-	-	-	-	-	0.875	0.640	-	-	-	-	0.597	-	-
Wo	-	-	47.9	47.2	-	-	-	-	-	-	46.5	46.0	-	-	-
En	-	-	45.7	39.2	-	-	-	-	-	-	39.4	39.1	-	-	-
Fs	-	-	6.4	13.6		-	-	-	-	-	14.1	14.9	-	-	-

	LV28-56-1-3									LV27-18/1					
	Cpx^{I}_{c}	Cpx^{I}_{r}	Cpx^{I}_{r}	Hb^{I}_{c}	Hb^{I}_{r}	Pl^{I}_{c}	Pl^{I}_{r}	Ol^{I}_{c}	Ol^{I}_{r}	Opx^{I}_{c}	Opx^{I}_{r}	Cpx^{I}_{c}	Cpx^{I}_{r}	Hb^{I}_{c}	Hb^{I}_{r}
SiO_2	52.45	51.20	50.96	42.35	40.22	45.71	48.46	39.84	39.41	54.63	55.85	52.08	53.19	42.29	42.42
TiO_2	0.45	0.70	0.85	1.93	2.04	n.d.	n.d.	0.00	0.00	0.16	0.16	0.50	0.29	2.50	2.21
Al_2O_3	3.32	4.16	3.91	12.77	13.19	35.14	32.81	0.00	0.00	1.56	1.26	2.80	1.86	12.45	12.70
Cr_2O_3	0.57	0.04	0.00	n.d.	n.d.	n.d.	n.d.	0.00	0.00	0.00	0.00	0.00	0.00	0.00	0.00
FeO	3.88	7.16	7.70	11.50	14.56	0.76	0.53	16.96	23.04	16.25	15.81	8.78	7.73	11.86	12.09
MnO	0.14	0.17	0.26	0.24	0.46	n.d.	n.d.	0.13	0.39	0.57	0.48	0.30	0.29	0.01	0.01
MgO	16.70	15.31	15.29	15.38	12.25	n.d.	n.d.	42.04	36.72	25.95	26.12	14.45	15.67	13.58	13.59
NiO	n.d.	n.d.	n.d.	n.d.	n.d.	n.d.	n.d.	n.d	n.d.	0.00	0.00	0.00	0.00	0.00	0.00
CaO	23.03	22.25	21.63	11.95	11.86	18.18	11.95	0.10	0.00	1.26	1.31	20.87	20.23	10.82	10.85
Na_2O	0.25	0.34	0.32	2.12	1.99	2.27	2.12	0.00	0.00	0.00	0.00	0.00	0.05	2.15	2.07
K_2O	0.02	0.00	0.00	0.83	0.92	0.15	0.83	0.00	0.00	0.00	0.00	0.00	0.00	0.10	0.11
Total	100.81	101.33	100.92	100.751	98.302	100.183	100.754	99.07	99.56	100.38	100.99	99.78	99.31	95.76	96.05
X_{Mg}	0.885	0.792	0.780	0.705	0.600	-	-	0.815	0.740	0.740	0.746	0.746	0.783	0.671	0.667
X_{An}	-	-	-	-	-	0.891	0.787	-	-	-	-	-	-	-	-
Wo	46.7	45.3	44.2	-	-	-	-	-	-	2.5	2.6	43.6	42.1	-	-
En	47.1	43.3	43.5	-	-	-	-	-	-	72.2	72.7	42.1	45.4	-	-
Fs	6.2	11.4	12.3	-	-	-	-	-	-	25.3	24.7	14.3	12.5	-	-

	LV27-18/1								LV28-48-1-1c						
	$Pl^{I}c$	$Pl^{I}r$	Ol^{II}	Opx^{II}	CPx^{II}_{c}	CPx^{II}_{r}	Hb^{II}_{r}	Ol^{I}_{c}	Ol^{I}_{r}	Cpx^{I}_{c}	Cpx^{I}_{r}	Hb^{I}_{c}	Hb^{I}_{r}	Pl^{I}_{c}	Pl^{I}_{r}
SiO_2	45.72	52.18	38.47	55.14	49.78	51.63	44.41	40.70	40.00	52.46	48.62	40.51	40.75	44.39	49.56
TiO_2	0.00	0.00	0.00	0.27	0.60	0.47	1.91	n.d.	n.d.	0.42	1.35	2.03	2.08	0.00	0.00
Al_2O_3	34.58	30.45	0.00	1.41	4.66	3.42	11.26	n.d.	n.d	3.74	6.22	15.02	14.42	36.24	31.15
Cr_2O_3	0.00	0.00	0.00	0.00	0.00	0.00	0.00	n.d.	n.d.	0.90	0.04	n.d.	n.d.	0.00	n.d.
FeO	0.51	0.71	24.16	15.88	8.89	8.50	12.51	10.63	15.31	3.93	7.87	10.60	11.05	0.22	0.66
MnO	0.00	0.00	0.51	0.52	0.17	0.20	0.15	n.d.	n.d.	0.14	0.15	0.18	0.18	n.d.	n.d.
MgO	0.01	0.01	36.89	25.21	13.42	14.47	14.00	48.61	44.82	16.65	13.75	14.81	14.44	n.d.	n.d.
NiO	0.00	0.00	0.00	0.00	0.00	0.00	0.00	0.20	0.18	0.00	0.00	n.d.	n.d.	n.d.	n.d.
CaO	17.34	12.68	0.00	1.50	21.52	20.62	10.90	n.d.	n.d.	22.92	22.15	12.77	12.79	19.26	14.40
Na_2O	1.29	3.86	0.00	0.00	0.03	0.06	2.11	n.d.	n.d.	0.31	0.45	2.13	2.12	0.73	2.94
K_2O	0.00	0.00	0.00	0.00	0.00	0.00	0.30	n.d.	n.d	0.00	0.02	1.08	1.05	0.02	0.21
Total	99.45	99.89	100.03	99.93	99.07	99.37	97.55	100.14	100.31	101.47	100.62	101.805	99.876	101.057	99.158
X_{Mg}	-	-	0.731	0.739	0.729	0.752	0.666	0.891	0.839	0.883	0.757	0.743	0.700	-	-
X_{An}	0.881	0.645	-	-	-	-	-	-	-	-	-	-	-	0.935	0.721
Wo	-	-	-	3.1	45.7	43.5	-	-	-	46.1	46.7	-	-	-	-
En	-	-	-	71.6	39.6	42.5	-	-	-	46.6	40.3	-	-	-	-
Fs	-	-	-	25.3	14.7	14.0	-	-	-	6.2	13.0	-	-	-	-

Note: Sample LV28-48-1f, LV28-56-1-3 – basalt, LV27-18/1 – basaltic andesite, LV28-48-1-1c – andesite. I – phenocrysts, II – microlites, c – core, r – rim, n.d. – not determined. X_{Mg}=Mg/(Mg+Fe), X_{An}=Ca/(Ca+Na+K). Total in addition included: 1 - F-1.62, Cl–0.06; 2 - F–0.71, Cl–0.10; 3 - BaO–0.08, SrO–0.06; 4 – BaO-0.13, SrO–0.05, 5 – F-2.65, Cl–0.02; 6 – F-0.98, Cl–0.01; 7 – BaO-0.08, SrO–0.11; 8 - BaO–0.15, SrO–0.08.

Major and trace elements

The analyzed samples from the Geophysicist seamount volcano range from basalt to andesite with SiO_2 47–60 wt. % and MgO 2.5-7.8 wt.% (Table 3, Fig. 2) and have geochemical features typical of the high-K calc-alkaline island-arc series. Like K, abundances of Rb, Sr and Ba are highly variable and comparable to similar rocks from other island arcs and also from the rear-arc zone of the Kurile Island Arc (Avdeiko et al., 1992). All samples have high La/Yb ratios (4.8–7.6) and show relative enrichment of large ion lithophile elements (Rb, Ba, U, Sr) and relatively depletion of high field strength elements (Nb, Ta, Zr, Hf).

The rocks from the Geophysicist volcano show characteristic depletion in Ta and Nb compared to large ion lithophile elements such as Th, K, Rb and La (Table 3, Fig. 3). Low Ni contents in the rocks (Table 3) suggest that they are not primary magma and have undergone olivine fractionation en route to the surface.

Rare earth elements

The rare earth element (REE) patterns on chondrite-normalized diagrams (Fig. 3a) show significant enrichment in the light REE's ($(La/Sm)_N$=1.57-2.76, $(La/Yb)_N$=3.51–5.25) and similar to those of island-arc lava from submarine volcanoes of the rear-arc zone of the Kurile Island Arc (Avdeiko at al., 1992). The pattern of several samples shows slight negative Eu anomalies as typical of arc volcanics.

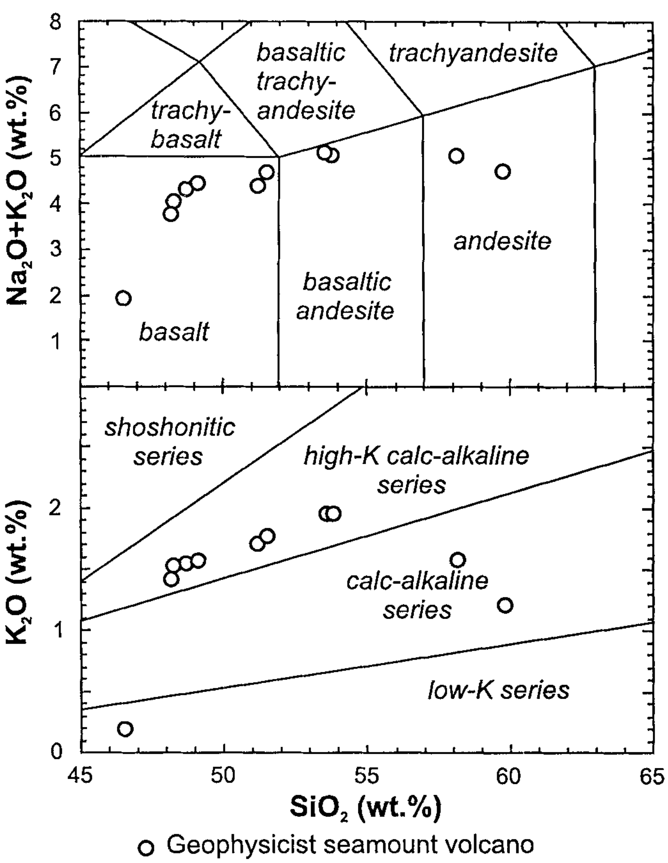

Fig. 2. SiO_2 – (Na_2O+K_2O) and SiO_2 – K_2O diagrams for volcanic rocks from the Geophysicist Seamount volcano.

Sr-Nd-Pb isotope ratios

Sr-Nd-Pb isotope ratios of most samples (N=8) from this seamount fall into the range of the Kurile island arc volcanoes (Table 4, Fig. 4, 5) (Bindemann and Bailey, 1999; Hoernle et al., 2000). These samples have $^{87}Sr/^{86}Sr$=0.70287–0.70342, $^{143}Nd/^{144}Nd$=0.51303–0.51308, $^{206}Pb/^{204}Pb$=18.38–18.40, $^{207}Pb/^{204}Pb$=15.48–15.51 and $^{208}Pb/^{204}Pb$=38.06–38.19 (Table 4). Several samples, however, extend to significantly higher $^{87}Sr/^{86}Sr$ (0.70378–0.70652; N=4) and to lower $^{143}Nd/^{144}Nd$ (0.51186–0.51262, N=3), $^{206}Pb/^{204}Pb$ (17.97–18.44, N=3) and $^{208}Pb/^{204}Pb$ (37.99–38.47, N=3) (Table 4). As it is evident from Fig. 4 and 5, these isotopic variations indicate assimilation of a continental crustal component, and thus, support the presence of thinned continental crust beneath the northeastern Kurile basin as has been suggested basing on petrological data (Tararin et al., 2000).

$^{87}Sr/^{86}Sr$ ratios of the Geophysicist volcano rocks correlate positively with Rb/Sr ratios (0.388 to 0.892) considering to be the result from assimilation of crustal rocks having different $^{87}Sr/^{86}Sr$ ratios and Sr concentrations (James, 1982).

Discussion

Available petrological and geochemical data indicate that high-K calc-alkaline rocks from the Geophysicist seamount volcano having a wide range of $^{87}Sr/^{86}Sr$ ratios (0.70287–0.70652; Table 4, Fig. 4) can not probably be explained by a simple fractional crystallization of a primary magma source modified by involvement of OIB-source (EM) mantle components. Satisfactory interpretation of trace element and Sr, Nd and Pb isotope geochemistry of volcanic rocks from this volcano requires involvement of the component derived from continental crustal materials.

Petrological and geochemical analyses of dredged rocks from the Geophysicist seamount indicate that this volcano shows some special features. High vesicularity of the rocks, as well as low sulfur concentrations in matrix glass (<400 ppm) compared to high sulfur contents of melt inclusion in phenocrysts (>2000 ppm) indicate volcanic activity in shallow water (<ca. 700 m) or subaerial conditions (Werner et al., 2000). Considering the available age data of the volcano (K-Ar age: 0.9 and 1.6 Ma; $^{40}Ar/^{39}Ar$ age: 0.84 and 1.07 Ma) and recent position of its summit in ca. 2300 m b.s.l., our data may imply extremely high

Table 3. Major and trace element analyses of volcanic rocks from the Geophysicist seamount volcano (data from Baranov et al., 2002).

	LV 28-48-1-3a	LV28-56-1-1	LV28-56-1-2	LV28-56-1-3	LV28-56-1-4	GE99-39/2	LV27-18/1	LV27-18/2	GE99-39/1	LV28-48-1-1c
SiO_2	48.05	48.92	50.36	48.23	48.99	51.03	54.47	54.64	57.69	60.58
TiO_2	0.92	0.95	0.85	0.94	0.95	0.91	0.73	0.74	0.80	0.61
Al_2O_3	17.06	17.98	16.67	17.74	17.82	18.01	18.31	18.46	17.12	15.07
Fe_2O_3	8.53	7.68	8.06	7.86	8.13	8.29	7.30	7.21	6.31	5.14
MnO	0.15	0.12	0.39	0.12	0.15	0.16	0.16	0.16	0.14	0.16
MgO	7.78	5.11	6.72	5.94	5.61	5.47	3.97	3.98	2.56	4.16
CaO	11.08	11.53	10.23	11.46	11.57	9.76	8.56	8.61	6.82	6.95
Na_2O	2.32	2.63	2.68	2.50	2.65	2.90	3.18	3.16	3.26	3.33
K_2O	1.41	1.94	1.66	1.52	1.52	2.19	2.03	1.94	1.90	1.12
P_2O_5	0.33	0.33	0.32	0.33	0.36	0.29	0.31	0.28	0.17	0.63
H_2O	1.02	n.d.	n.d.	1.40	n.d.	1.05	1.69	1.64	1.57	n.d.
LOI	n.d.	1.93	1.53	n.d.	1.58	1.10	1.74	1.64	1.76	1.14
CO_2	0.14	n.d.	n.d.	0.08	n.d.	0.03	0.07	0.05	0.52	n.d.
Total	98.79	99.12	99.47	98.12	99.33	100.09	100.78	100.87	98.86	98.89
Rb	20	32	32	27	27	43	47	50	26	21
Sr	516	492	469	540	457	520	549	561	430	365
Ba	366	313	394	319	287	343	371	396	426	341
Y	24	219	20.8	25	20.9	22.7	20.4	20.8	26.4	20
Sc	n.d.	44	39	n.d.	43	40	24	23	17	26
Zr	70	70	92	78	61	75	86	90	160	75
Co	34	25	22	34	19	24	15	17	12	10
Ni	93	59	60	96	47	38	17	19	12	24
Cr	188	239	224	172	229	78	32	20	<18	99
V	288	284	250	296	264	324	212	220	139	143
Cu	n.d.	72	50	n.d.	38	56	33	41	19	24
Zn	n.d.	62	49	67	-	63	68	92	48	-
Pb	<40	10	23	<4	16	16	6	12	25	25
Sb	n.d.	0.3	0.3	n.d.	-	-	-	-	0.2	0.2
Ga	15	18	16	15	14	19	17	18	17	12
Ge	n.d.	1.8	1.6	n.d.	1.1	2.0	1.8	2.0	1.5	1.3
Nb	4	26	3.5	5	2.2	2.5	2.7	2.9	5.3	2.4
Cs	n.d.	1.5	1.2	n.d.	1.1	1.8	2.2	2.4	0.6	1.0
La	<14	10.4	14.1	<14	10.5	12.2	14.1	14.5	19.1	9.86
Ce	20	24.9	30.2	51	24.2	27.5	31.2	31.9	40.7	21.9
Pr	n.d.	3.46	3.90	n.d.	3.43	3.78	4.07	4.28	4.92	2.83
Nd	4	16.5	17.4	n.d.	16.4	17.8	18.2	18.7	19.5	12.6
Sm	n.d.	4.15	3.95	n.d.	3.97	4.27	4.08	4.10	4.30	3.00
Eu	n.d.	1.46	1.35	n.d.	1.37	1.48	1.38	1.37	1.19	1.04
Gd	n.d.	4.47	4.22	n.d.	4.28	4.52	4.29	4.25	4.68	3.42
Tb	n.d.	0.66	0.59	n.d.	0.66	0.68	0.59	0.62	0.72	0.51
Dy	n.d.	3.67	3.32	n.d.	3.54	3.82	3.32	3.36	4.25	3.09
Ho	n.d.	0.77	0.67	n.d.	0.72	0.77	0.69	0.69	0.90	0.68
Er	n.d.	2.18	1.94	n.d.	2.10	2.25	1.93	2.07	2.62	1.95
Tm	n.d.	0.316	0.282	n.d.	0.304	0.338	0.292	0.305	0.390	0.299
Yb	n.d.	2.05	1.86	n.d.	1.95	2.18	1.99	2.05	2.62	2.06
Lu	n.d.	0.317	0.290	n.d.	0.299	0.325	0.323	0.325	0.406	0.321
Hf	n.d.	1.8	2.2	n.d.	1.6	2.0	2.1	2.2	3.9	2.0
Ta	n.d.	0.1	0.2	n.d.	0.1	0.1	0.2	0.2	0.3	0.2
Th	6	1.85	2.56	10	1.66	2.28	2.72	2.79	4.38	1.93
U	n.d.	0.88	0.78	n.d.	1.88	0.81	1.01	1.06	1.15	0.63
Tl	n.d.	0.50	0.44	n.d.	0.17	0.22	0.26	0.34	0.11	-

Note: Total iron as Fe_2O_3. Inductively coupled plasma spectrometry (major elements) for Samples LV-56-1-1, LV56-1-2, LV56-1-4, GE99-39/1, GE99-39/2, LV27-18/1, LV27-18/2, LV48-1-1c. X-ray fluorescence analyses (major and trace elements) for Samples LV48-1-3a, LV56-1-3. Inductively coupled plasma and mass spectrometry (trace elements) for Samples LV-56-1-1, LV56-1-2, LV56-1-4, GE99-39/1, GE99-39/2, LV27-18/1, LV27-18/2, LV48-1-1c. H_2O and CO_2 were determined by spectrophotometer.

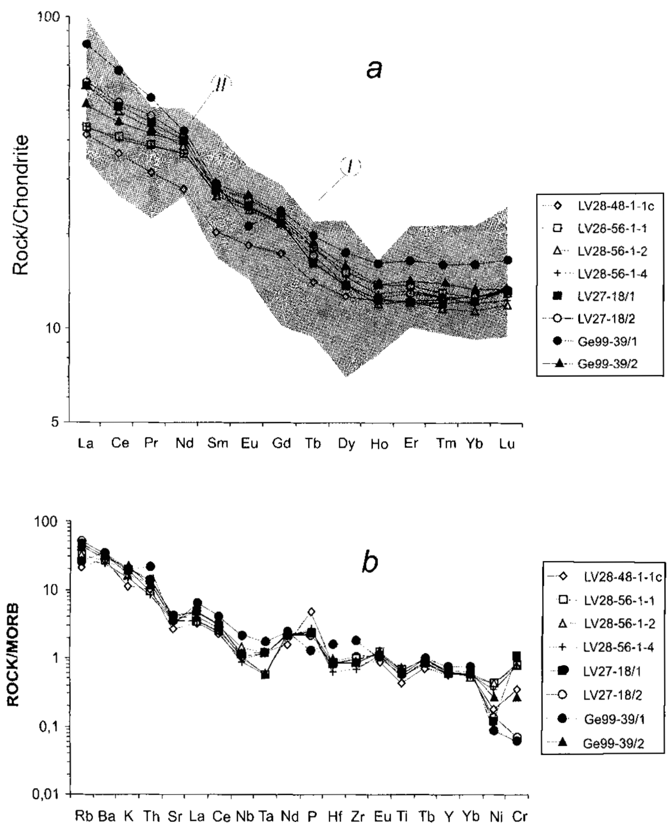

Fig. 3. Chondrite-normalized (Anders and Grevesse, 1989) REE pattern (a) and MORB-normalized (Saunders and Tarney, 1984) spider diagram (b) for the volcanic rocks from the Geophysicist Seamount volcano. Fields for representative whole rock samples from the front (I) and rear-arc (II) zones of the Kurile Island Arc (Avdeiko et al., 1992) are shown for comparison on REE's diagram.

subsidence rates (1-2 mm/a) for the eastern Kurile Basin (Baranov et al., 2002).

Large thickness of sediments (ca. 3–4.5 km), almost completely obscuring the basement structure has resulted in controversial opinions on the Kurile Basin origin. Snegovskoy (1974) considers the basin to be a relic block of oceanic plate or the old Okhotsk oceanic plateau (Bogdanov and Dobretsov, 2002) or a downwarping zone at the edge of the Okhotsk continental plate (Belousov and Udintsev, 1981). The alternative opinions prevail, however. According to them the Kurile Basin is a new back-arc basin being formed: (a) by spreading, caused by subduction of the Pacific Plate under Kurile Islands (Bogdanov, 1988), (b) by continental rifting, crustal thinning and break-up of continental crust, coeval with sinistral NE strike-slip motion (Utkin, 1984), (c) by continental rifting and coeval clockwise rotation that form a pull-apart basin (Baranov et al., 1999; 2002).

At present, none of these hypotheses can be considered reasonable without deep-sea drilling data. The active tectonic and magmatic processes in the Kurile Basin, however, are doubtlessly active; they are evident from the high heat flow values, the anisotropic structure of the upper mantle and recent volcanism.

Conclusion

The Kurile Basin is the greatest and deepest basin of the Okhotsk Sea. The dredging program under KOMEX Russian-Germany Project was carried out on the Geophysicist seamount volcano in the northeastern part of the Kurile Basin where pillow-like lavas, brecciated and even scoriaceous fragments of highly porphyritic and highly vesiculated basalt, basaltic andesite and andesite have been sampled. Geochemistry of the rocks is typical of high-K island-arc volcanism. They are enriched in LILE and depleted in Zr, Ti, Nb, Ta and Y. The REE patterns are characterized by enrichment in LREE, similar to those of island-arc lava from submarine volcanoes of rear-arc zone of the Kurile Island Arc.

The available petrological and geochemical data indicate that the rocks from the Geophysicist seamount have a wide range of $^{87}Sr/^{86}Sr$ ratios (0.70287-0.70652) that can not be explained by a simple fractional crystallization of primary basic magma modified by OIB-source mantle component. The only satisfactory interpretation of the trace element and Sr, Nd, Pb geochemistry of rocks requires involvement of the components derived from continental crustal materials. Thus we propose that the basement of the northeastern

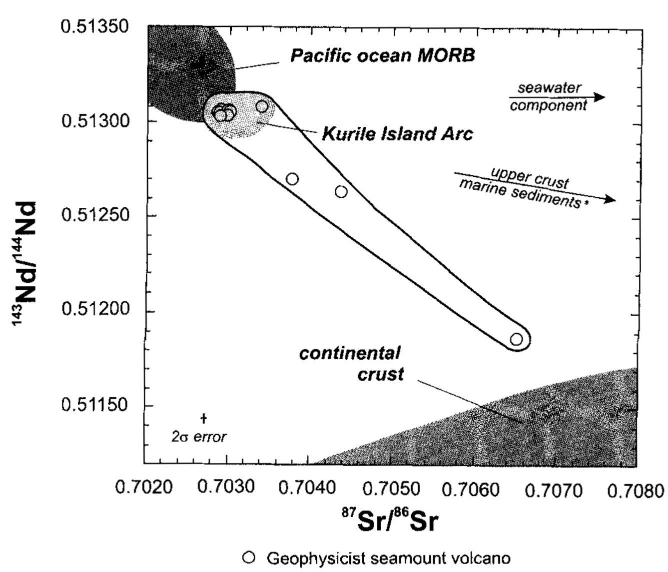

Fig. 4. $^{87}Sr/^{86}Sr$ – $^{143}Nd/^{144}Nd$ isotope ratios for volcanic rocks from the Geophysicist Seamount volcano. Arrow points at bulk composition of sediments at the Kurile Trench (Plank and Langmuir, 1998).

Table 4. Isotopic data for Sr, Nd, and Pb in Samples from the Geophysicist seamount volcano (data from Baranov et al., 2002).

Sample	$^{87}Sr/^{86}Sr \pm 2\sigma$	$^{143}Nd/^{144}Nd \pm 2\sigma$	$^{143}Nd/^{144}Nd_N \pm 2\sigma$	$^{206}Pb/^{204}Pb_N$	$^{207}Pb/^{204}Pb_N$	$^{208}Pb/^{204}Pb_N$
LV28-48-1-3a	0.702953±8	0.513043±10	0.513048±10	18.389	15.485	38.101
LV28-56-1-1	0.702934±7	0.513035±9	0.513039±9	18.397	15.491	38.116
LV28-56-1-2	0.703764±7	0.512699±13	0.512703±13	17.969	15.505	37.998
LV28-56-1-3	0.702940±10	0.5130040±4	0.513045±4	18.396	15.491	38.115
LV28-56-1-4	0.702945±7	0.513046±6	0.513049±6	18.403	15.494	38.122
GE99-39/2	0.702876±9	0.513026±5	0.513046±5	18.395	15.492	38.11
GE99-39/6	0.703424±8	0.513076±9	0.513096±9	18.380	15.508	38.194
LV27-18/1	0.702874±7	0.513026±4	0.513036±4	18.391	15.478	38.063
LV27-18/2	0.702870±7	0.513029±7	0.513040±7	18.395	15.480	38.071
GE99-39/1	0.706519±8	0.512234±9	0.511877±9	18.056	15.463	38.337
LV28-48-1-1c	0.704424±7	0.512616±6	0.512619±6	18.442	15.492	38.467

Kurile Basin, presently at ~6 km depth, is likely to represent thinned continental crust.

Acknowledgments

We are grateful to the Shipboard Scientific Parties and the crews of the R/V 'Akademik Lavrentyev' (27, 28 cruises) and HV 'Marshal Gelovany' (99 cruise) for their help in acquiring the samples used in this study. We are also grateful to German Ministry of Education and Research (BMBF; Grant KOMEX I) and Russian Ministry of Industry and Science (MPN; Grant KOMEX I) for the funds they supported this study with.

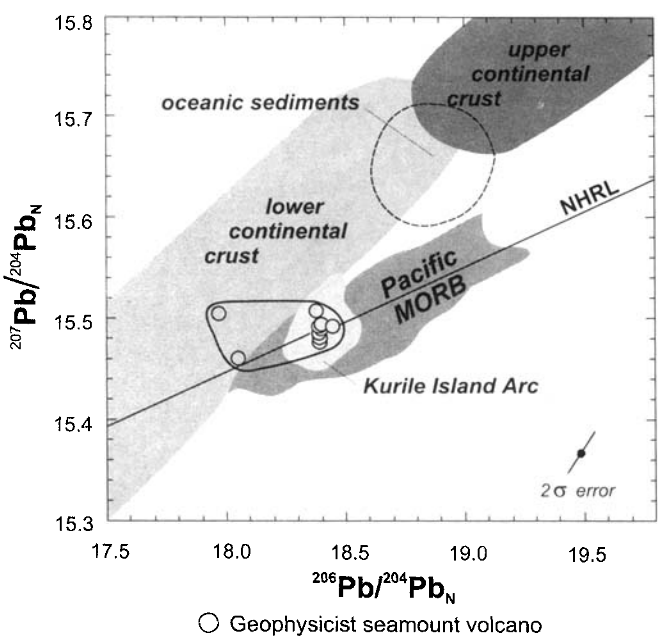

Fig. 5. Pb isotope ratios. NHRL–Northern Hemisphere Reference Line (Hart, 1984). Fields: for continental crust (Wilson, 1989), for Pacific MORB (Hickey-Vargas, 1998), marine sediments (Elliott et. al., 1997; Pearce et al., 1999; Plank and Langmuir, 1998).

References

Anders, E. and Grevesse, N. (1989) Abundances of the elements: meteoritic and Solar. Geochem. Cosmochim. Acta, v. 53, pp. 197-214.

Avdeiko, G.P., Antonov, A.Yu., Volynetz, O.N., Bondarenko, V.I., Rashidov, V.A., Tsvetkov, A.A., Gladkov, N.G., Markov, I.A. and Paluyeva, A.A. (1992) Submarine volcanism and zonality of the Kuril island arc. Nauka, Moscow, 528 p, (in Russian).

Baranov, B.V., Dozorova, K.A., Karp, B.Ya. and Karnaukh, V.A. (1999) Geometry of the Kurile Basin opening. Doklady Akademii Nauk Russia, v. 367, pp. 376-379 (in Russian).

Baranov, B.V., Werner, R., Hoernle, K.A., Tsoy, I.B., van den Bogaard, P. and Tararin, I.A. (2002) Evidence for compressionally-induced high subsidence rates in the Kurile Basin (Okhotsk Sea). Tectonophys., v. 350, pp. 63-97.

Belousov, V.V. and Udintsev, G.B. (Eds.), (1981) Seafloor structure of the Okhotsk Sea. Nauka, Moscow, 176p. (in Russian).

Biebow, N. and Hütten, E. (Eds.), (1999) Cruise reports: KOMEX I and II. RV Prof. Gagarinsky cruise 22, RV Akademik Lavrentyev cruise 28. GEOMAR Report 82, 188p.

Biebow, N., Lüdmann, T., Karp, B. and Kulinich, R. (Eds.), (2000) Cruise Reports: KOMEX V and VI, GEOMAR Report 88, Kiel, 296p.

Bikkenina, S.K., Anosov, G.I., Argentov, V.V. and Sergeev, K.F. (1987) Crustal structure of the southern Okhotsk Sea according to seismic refraction data. Nauka, Moscow, 86p (in Russian).

Bindemann, I.N. and Bailey, J.C. (1999) Trace elements in anorthite megacrysts from the Kurile Island Arc: a window to across-arc geochemical variation in magma compositions. Earth Planet. Sci. Lett., v. 169, pp. 209-226.

Bogdanov, N.A. (1988) Tectonics of backarc basins from marginal seas. Nauka, Moscow, 221p. (in Russian).

Bogdanov, N.A. and Dobretsov, N.L. (2002) The Okhotsk volcanic oceanic plateau. Geologia i Geofizika, v. 43, pp. 101-114.

Elliot, T., Plank, T., Zindler, A., White, W. and Bourbon, B. (1997) Element transport from slab to volcanic front at the Mariana arc. J. Geophys. Res., v. 102, pp. 14991-15019.

Frolova, T.I., Perchuk, L.L. and Burikova, I.A. (1989) Magmatism and transformation of the crust from the active continental margins. Nauka, Moscow, 261p, (in Russian).

Geodekyan, A.A., Udintsev, G.B., Baranov, B.V., Bersenev, A.F., Berk, K., Bogatikov, O.A., Gabov, V.V., Gnibidenko, G.S., Dmitriev, Yu.I., Zonenshain, L.P., Kurentsova, N.A., Raznitsin, Yu.N., Rudnik, G.B. and Sushchevskaya, N.M. (1976) Bedrocks of the central Okhotsk Sea. Sovetskaya Geologia, v. 6, pp. 12-31, (in Russian).

Gnibidenko, G.S. (1979) Tectonics of the seafloor from the east marginal seas. Nauka, Moscow, 163p, (in Russian).

Gnibidenko, H.S., Hilde, T.W.C., Gretskaya, E.V. and Andreev, A.A. (1995) Kurile (South Okhotsk) back-arc basin. In: Taylor, B. (Ed.), Back-arc basins: tectonics and magmatism. Plenum Press, New York, pp. 421-449.

Gnibidenko, H.S. and Svarichevsky, A.S. (1984) Tectonics of the South Okhotsk deep-sea basin. Tectonophys., v. 102, pp. 225-244.

Hart, S.R. (1984) A large-scale isotope anomaly in the Southern Hemisphere mantle. Nature, v. 309, pp. 753-757.

Hayashi, T. (1997) The study of thermal structure and tectonic history of the Derugin Basin, Sea of Okhotsk. Master's Thesis, Earthquake Research Institute, University of Tokyo, 39p.

Hickey-Vargas, R.L. (1998) Origin of the Indian Ocean-type isotopic signature in basalts from Philippine Sea plate spreading centers: an assessment of local versus large-scale processes. J. Geophys. Res., v. 103, pp. 20963-20980.

Hoernle, K. and Tilton, G. (1991) Sr-Nd-Pb isotope data for Fuerteventura (Canary Islands) basal complex and subaerial volcanic: applications to magma genesis and evolution. Schweizer Mineral. und Petrograph. Mitteilungen, v. 71, pp. 5-21.

Hoernle, K., Werner, R., Volynets, O., Avdeiko, G., Schmidt, A., Wenskowski, B., Doubik, P. and Tararin, I.A. (2000) Magma genesis beneath the Kurile Island arc: the fundamental role of fluids in subduction zones. Third Workshop on Russian – German Cooperation in the Okhotsk Sea – Kurile Island arc system (KOMEX). Program and Abst. Moscow, p. 31.

Ikeda,Y., Stern, R., Kagami, H. and Sun, Ch.-H. (2000) Pb, Nd, and Sr isotopic constraints on the origin of Miocene basaltic rocks from northeast Hokkaido, Japan: implications for opening of the Kurile back-arc basin. The island arc, v. 9, pp. 161-172.

James, D.E. (1982) A combined O, Sr, Nd, and Pb isotopic and trace element study of crustal contamination in Central Andean lavas, I. Local geochemical variations. Earth Planet. Sci. Lett., v. 57, pp. 47-62.

Kharakhinov, V.V. (1996) Tectonics and development history of the sedimentary basins. In: Rodnikov, A.G., Tuezov, I.K., Kharakhinov, V.V. (Eds.), Structure and dynamics of the lithosphere and asthenosphere of the Okhotsk region. Russian Academy of Sciences, Moscow, pp. 256-305 (in Russian).

Kimura, G. and Tamaki, K. (1986) Collision, rotation, and back-arc spreading in the region of the Okhotsk and Japan Seas. Tectonics, v. 5, pp. 386-401.

Leake, B.E. (1978) Nomenclature of amphiboles. Canad. Mineral., v. 16, p. 501-520.

Lelikov, E.P. (1992) Metamorphic complexes of the marginal seas of the Pacific. Dal'nauka, Vladivostok, 168p. (in Russian).

Neprochnov, Yu.P., Semenov, G.A. and Hao Tinyao (1999) Seismogravity modeling of the Okhotsk Sea earth's crust. Oceanology, v. 39, pp. 622-627 (in Russian).

Nürnberg, D., Baranov. B. and Karp, B. (Eds.), (1997) RV Akademik M.A.Lavrentyev cruise 27 – cruise report Gregory. GEOMAR Report 60, 69p.

Pearce, J.A., Kempton, P.D., Nowell, G.M. and Noble, S.R. (1999) Hf-Nd element and isotope perspective on the nature and provenance of mantle and subduction components in western Pacific arc-basin systems. J. Petrol., v. 40, pp. 1579-1611.

Plank, T. and Langmuir, C.H. (1998) The chemical composition of subducting sediment and its consequences for crust and mantle. Chem. Geol., v. 145, pp. 325-394.

Saunders, A.D. and Tarney, J. (1984) Geochemical characteristics of basaltic volcanism within back-arc basins. In: Kokelaar, B.P., Howells, M.F. (Eds.), Marginal Basin Geology. Volcanic and associated sedimentary and tectonic processes in modern and ancient marginal basins. Geol. Soc. Blackwell Sci. Publ. Oxford London Edinburg Boston Palo Alto Melbourne, pp. 59-76.

Sergeev, K.F., Zverev, S.M. and Veitsman, P.S. (Eds.) (1987), Geologic-geophysical atlas of the Kurile-Kamchatka Island Arc. VSEGEI, Leningrad.

Snegovskoy, S.S. (1974) Seismic reflection investigations and tectonics of the southern Okhotsk Sea and adjacent areas of Pacific. Novosibirsk, Nauka, 104p. (in Russian).

Takeuchi, T., Kodama, K. and Ozawa, T. (1999) Paleomagnetic evidence for block rotations in central Hokkaido-south Sakhalin, Northeast Asia. Earth Planet. Sci. Lett., v. 169, pp. 7-21.

Tararin, I.A., Lelikov, E.P. and Itaya, T. (2000) Pleistocene submarine volcanism of the eastern part of the Kurile Basin (Okhotsk Sea). Doklady Akademii Nauk, v. 371, pp. 366-370 (in Russian).

Todt, W., Cliff, R.A. and Hanser, A. (1996) Evalution of a 202Pb-205Pb double spike for high precision lead isotope analyses. In: Basu, A. and Hart, S. (Eds.), Earth processes. Reading the isotopic code, AGU, Washington, Geophys. Monograph, v. 95, pp. 429-437.

Utkin, V.P. (1984) Geodynamic conditions of the formation of marginal-continental volcanic belts. In: Shcheglov, A.D. (Ed.), Volcanic belts of Eastern Asia. Moscow, Nauka, pp. 328-352.

Werner, R., Tararin, I.A., Doubik, P., Hoernle, K. and Lelikov, E.P. (2000) Submarine volcanism in the north-eastern part of the Kurile Basin: implications for crustal structure and geodynamic evolution. Third Workshop on Russian-German cooperation in the Okhotsk Sea-Kurile island arc system KOMEX. Program and abst. Moscow, April 17-20, 2000, pp. 59-60.

Wilson, M. (1989) Igneous petrogenesis. A global tectonic approach. Unwin Hyman, London Boston Sydney Wellington, 466p.